AD_____

Award Number: **W81XWH-07-1-0716**

TITLE: **Neuroprosthetics and Solutions for Restoring Sensorimotor Functions**

PRINCIPAL INVESTIGATOR: Douglas Weber, Ph.D.

CONTRACTING ORGANIZATION: University of Pittsburgh

Pittsburgh, PA 15260

REPORT DATE: December 2009

TYPE OF REPORT: Annual Report

PREPARED FOR: U.S. Army Medical Research and Materiel Command
Fort Detrick, Maryland 21702-5012

REPORT DOCUMENTATION PAGE

Form Approved
OMB No. 0704-0188

1. REPORT DATE *(DD-MM-YYYY)*	2. REPORT TYPE	3. DATES COVERED *(From - To)*
01-12-2009	Annual	26 SEP 2008 - 30 NOV 2009

4. TITLE AND SUBTITLE
Neuroprosthetics and Solutions for Spinal Cord Dysfunctions

5a. CONTRACT NUMBER

5b. GRANT NUMBER
W81XWH-07-1-0716

5c. PROGRAM ELEMENT NUMBER

6. AUTHOR(S)
Douglas Weber, PhD, PI
Carl Lagenaur, PhD, Co-I
Wei Wang, PhD, Co-I
Rory Cooper, PhD, Co-I
Tracy Cui, PhD, Co-I

5d. PROJECT NUMBER

5e. TASK NUMBER

5f. WORK UNIT NUMBER

7. PERFORMING ORGANIZATION NAME(S) AND ADDRESS(ES)
University of Pittsburgh
Pittsburgh, PA 15260

8. PERFORMING ORGANIZATION REPORT NUMBER

9. SPONSORING / MONITORING AGENCY NAME(S) AND ADDRESS(ES)
U.S. Army Medical Research
Fort Detrick, Maryland

10. SPONSOR/MONITOR'S ACRONYM(S)

11. SPONSOR/MONITOR'S REPORT NUMBER(S)

12. DISTRIBUTION / AVAILABILITY STATEMENT
Approved for public release; distribution unlimited

13. SUPPLEMENTARY NOTES

14. ABSTRACT

This project is focused on the development of a radically new class of prosthetic devices that will mimic more closely the full range of sensory and motor capabilities of natural limbs. To this end, we have made initial progress on four integrated projects to advance the development of neuroprosthetic limbs including: 1) creation of a sensory neural interface to provide amputees with tactile and kinesthetic feedback from their prosthetic limb, 2) improving the biocompatibility of implanted neural interface electrodes, 3) development of a virtual reality training and testing system for neuroprosthetic limbs, and 4) development of prosthetic hardware testing equipment and procedures. To date, we have completed pilot experiments to characterize the organization of sensory neurons in the DRG for the creation of a sensory feedback neural interface and evaluated the brain's response to sensory stimulation. We have completed pilot experiments to evaluate histologically the tissue response to electrodes implanted chronically in DRG, dorsal roots, and spinal cord. We have designed and developed a virtual reality training system based on BCI2000, creating custom software to greatly extend the functionality of BCI2000. Finally, we have developed a test jig to determine compliance with ISO standards for prosthetic hardware, and we have begun testing prosthetic feet.

15. SUBJECT TERMS
neural interface, neural prosthesis, biocompatibility, virtual reality, amputee, sensory feedback

16. SECURITY CLASSIFICATION OF:			17. LIMITATION OF ABSTRACT	18. NUMBER OF PAGES	19a. NAME OF RESPONSIBLE PERSON
a. REPORT	b. ABSTRACT	c. THIS PAGE			USAMRMC
U	U	U	UU	27	19b. TELEPHONE NUMBER *(include area code)*

TABLE OF CONTENTS

Introduction

Advances in body armor and life-saving technology have increased survival rates of severely injured military personnel. Unfortunately, the survivors of improvised explosive devices used in gulf conflicts are often left with amputations and/or spinal cord injuries. The increase in amputations and paralysis among military personnel requires significant advances in prosthetics and functional electrical stimulation (FES) systems such that the soldiers can return to the field if they desire or to productive civilian lives. This project is focused on the development of a radically new class of prosthetic devices that will mimic more closely the full range of sensory and motor capabilities of natural limbs. By providing a communication link between the prosthesis and the user's nervous system, our goal is to integrate the prosthetic limb as a natural component of the user's sensorimotor apparatus. Significant progress has been made toward this goal, but there is still much work to be done, particularly in the areas of restoring sensory feedback, improving the electrode-neuron interface, user-training, and prosthetic durability. **Project 1** deals directly with the issue of providing somatosensory input to soldiers with amputation or paralysis. **Project 2** deals with improving the chronic stability of the neural interface and will test novel polymer surface modification methods for improving the long-term reliability of the implanted microelectrodes. Although neural control is the ultimate goal of our work, we believe that there is useful control information available in the muscles of the residual limb. **Project 3** uses virtual reality to place patients in an environment with a simulated neuroprosthesis. In this environment, we can discover the degree of remaining electromyographic (EMG) signal content and begin to train patients to control their neuroprosthetic. In this way, the virtual environment serves two important purposes: 1) testing algorithms for myoelectric and/or neural control, and 2) training the user on neuroprosthetic control. This new class of prosthetic devices will literally look, feel, and function like natural limbs, but their internal construction will include complex machinery, motors, sensors, and control instrumentation. Therefore, durability is a major concern, especially since users will be more able to engage in rigorous physical activities. Through our interactions with soldiers returning to duty after amputation, we know that current prosthetics do not stand up to the harsh use of active amputees. **Project 4** is designed to rigorously test currently available and newly design prosthetics to understand the components that fail and the ways to remediate these failures. In addition, we will build devices that can track prosthetic use and thus provide information on the use in terms of both distance traveled and force imparted.

Body

Project 1. Develop a somatosensory neural interface (SSNI)

The overall goal of project 1 is to restore natural sensations of limb posture and movement through multichannel microstimulation of the normal afferent pathways involved in proprioception. Two objectives must be met to achieve this overall goal. First, we must identify an appropriate location in the somatosensory nervous system for implanting microelectrode arrays to stimulate primary afferent (PA) neurons. We are examining the somatotopic organization and recruitment of primary afferent fibers in the DRG, dorsal root, and dorsal root entry zone to develop a technique called primary afferent microstimulation (PAMS). Multichannel PAMS is used to generate a spatiotemporal pattern of sensory input that encodes limb-state information for the whole limb. Neural recordings in primary somatosensory cortex are used to evaluate the response in the brain, and evaluate the effectiveness of various inputs.

In the first year of this project, we characterized the stimulation threshold for recruiting PA fibers (Gaunt, 2009) and have developed a computational model to provide a theoretical framework for further exploration (Bourbeau, 2008). We have also begun studies to evaluate the brain's response to PAMS (Hokanson, 2009). This portion of animal testing was performed in conjunction with a related NIH funded project – no animal testing with cats was performed with TATRC funds. A new animal protocol has been submitted to our local IACUC to pursue experiments that are specific to and funded by the TATRC project. An ACURO protocol application will be submitted upon approval of the IACUC protocol (see 'Plans' section).

A more complete summary of these results is provided below. In the second year of this project, we are extend this work to test the long-term reliability of the neural interface in awake, behaving cats. Electrodes will be implanted chronically in the DRG and/or adjacent dorsal roots. Neural recordings in the brain will be made during PAMS while the cat is standing or walking (see 'Plans' section).

Results

Recruitment of PA neurons by DRG microstimulation

Experiments were performed to determine the minimum current (i.e. threshold) required to excite PA neurons in the DRG and to determine the effect of fiber diameter on the recruitment threshold. Across all cats (n=4), the threshold stimulus amplitude was 2.7 ±

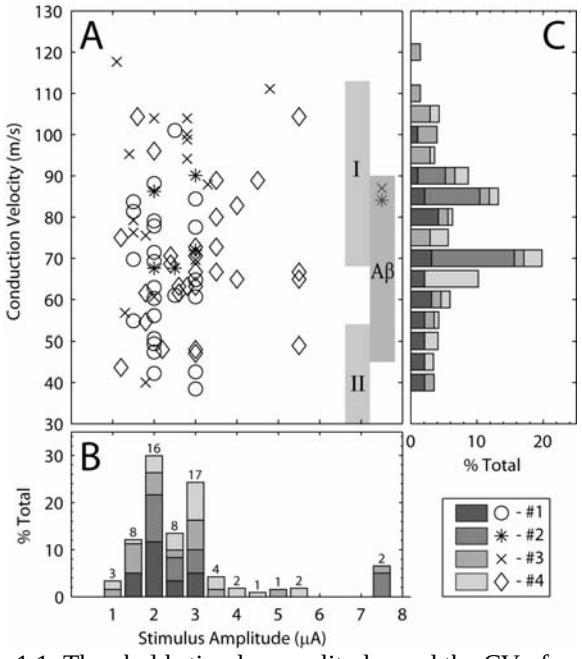

Figure 1.1: Threshold stimulus amplitudes and the CV of afferents recruited by microstimulation in the DRG. The legend identifies the data for each animal. (A) CV and stimulus amplitude for threshold responses. (B) Histogram of the threshold amplitude for all electrodes, normalized by the total number of electrodes in each animal. (C) Histogram of CVs at threshold normalized by the total number of electrodes in each

1.3 µA (mean±standard deviation). The lowest stimulus amplitude that elicited a response was 1.1 µA and in 76% of the cases, the threshold stimulus amplitude was less than or equal to 3 µA. It was found that the conduction velocities (CV) of fibers recruited at threshold ranged from 38 m/s to 118 m/s, indicating that a wide range of fiber diameters can be recruited selectively at the low intensities of stimulation used in the DRG. Figure 1.1 summarizes these results in terms of the threshold stimulation amplitude and the CVs measured at threshold for each electrode. Panel A shows a scatter plot of CVs and stimulus amplitudes for all threshold responses. Panel B shows a normalized histogram of the stimulation thresholds and panel C shows a normalized histogram of the CVs of units recruited at threshold on each electrode. Two distinct peaks in the measured CVs were observed at approximately 85 m/s and 70 m/s. These correspond to the median CV of axons in the group I range (~85 m/s) and Aβ range (~72 m/s). A complete report of this study has been published (Gaunt, 2009). ***The key point of this figure is that PA neurons from a range of sensory modalities can be recruited at low stimulation intensities in the DRG.***

The in vivo studies have provided important insights into the electrical stimulation requirements for activating PA. In particular, we were surprised to find that about half the time, PAMS recruited medium diameter fibers before large diameter fibers at the low range of stimulation intensities that were used. In contrast, large diameter fibers are recruited preferentially with extraneural stimulation, which generally requires higher intensity stimulation. We hypothesized that because the electrodes were placed in close proximity to the fibers, the dominant factor in determining recruitment is distance to the nearest node of Ranvier, rather than the intensity of current. Furthermore, since there are generally fewer large diameter fibers compared to the medium and smaller diameter fibers, the likelihood of recruiting medium diameter fibers is increased. To test this hypothesis, we created a computational model explore the effect of electrode proximity (to nearest node of Ranvier) on stimulation threshold. This model was also used to study recruitment (i.e. number of fibers activated) at increasing intensities of stimulation. Figure 1.2A shows that as the stimulus amplitude increases, the electrode-to-node distance increases for all fiber diameters. However, the relative distance is nearly the same for all fibers when the stimulation intensity is less than 10 µA – at higher intensities, the electrode needs to be closer to the smaller diameter fibers. This distance is used to define a 'sphere-of-activation' for each combination of fiber type and stimulation intensity (Figure 1.2B). This sphere is used to estimated how many fibers of each type will be activated for a given intensity, because all fibers having a node within the sphere will be recruited. We are using this model to simulate the recruitment of PA neurons over a range of conditions, including varying the density and distribution of fibers in the DRG and dorsal roots. This analysis will be useful for designing an electrode configuration that will enable selective recruitment of PA fibers.

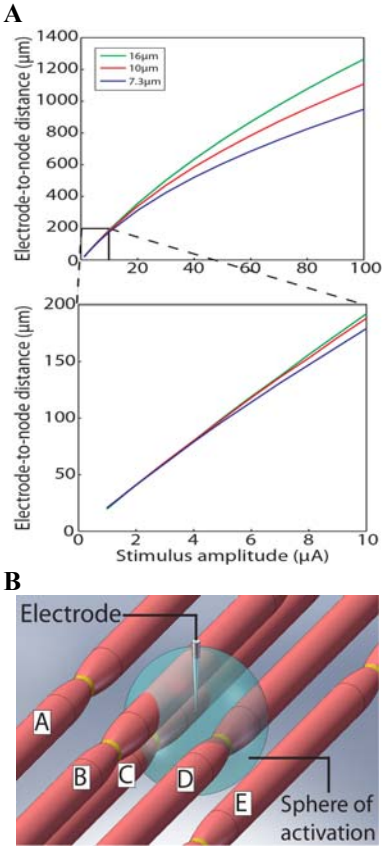

Figure 1.2: A) minimum electrode-to-node distance required to activate fibers at increasing stimulus intensities. B) Sphere of activation (radius) as defined by electrode-to-node distance allows analysis of number and type of fibers that are recruited.

Response of S1 to PAMS patterned from neural data recorded during passive movement

Experiments have been performed to record simultaneously from large numbers of neurons in DRG and S1 during passive movement of the hindlimb. Figure 1.3 shows an example of modulated activity of a single DRG neuron and a single S1 neuron during passive movement of the hindlimb mimicking stepping. The spike rasters and firing rates for both neurons display activity that covaries strongly with ankle joint angle, demonstrating that these neurons may encode proprioceptive information for the ankle. In general, up to 100 electrodes in both the DRG and cortex are recorded simultaneously, many of which exhibit similar modulated activity. ***The key point of this figure is that the time-varying activity of DRG PA neurons and S1 cortical neurons conveys specific proprioceptive information about the mechanical state of the limb.***

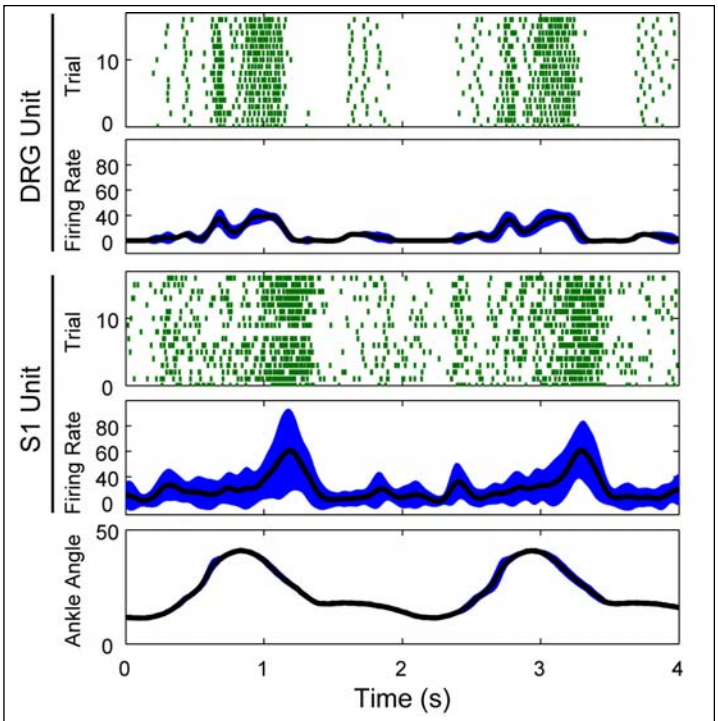

Figure 1.3: Spike rasters and binned firing rates (50 ms bins) for a DRG and S1 unit recorded simultaneously in response to robot generated stepping. Two step cycles are displayed. Kinematics and firing rates are shown as the mean (black line) ± SD (blue). Note that the DRG and S1 responses are modulated by the kinematics.

One method to deliver surrogate somatosensory information to S1, is to pattern PAMS stimulation on PA activity recorded during natural movements. We refer to this as 'replay' PAMS, since the goal is to simulate the natural pattern of PA input that is observed during limb movement. We have demonstrated that cortical activity recorded during center-out movements and corresponding replay stimulation is comparable. Figure 1.4 shows an example. A group of 34 neurons were recorded in S1, and 13 of these were highly correlated ($R^2 > 0.5$) with foot-speed, indicating that they were modulated by the movement condition. Panel A in Figure 1.4 shows an example of the similarity in the response of an S1 neuron during the movement (green) and replay (blue) conditions. While the replay response does not reproduce all of the natural responses in this neuron, it is clear that at least some portions of the movement-evoked response in S1 were reproduced by the replay stimulation. Since many of the S1 neurons were highly correlated with foot speed, it was possible to build a neural decoder that estimated foot speed from S1 activity. Panel B shows that the decoder is highly accurate ($R^2 = 0.92$) in predicting foot speed (black trace) during the movement condition (green trace) and that the neural activity recorded during the replay condition also enabled a good estimate of foot speed ($R^2 = 0.52$, blue trace).

We also tested the effects of varying the stimulation intensity and replay pulse-rate on the accuracy of decoding limb-state information activity from S1 (Figure 1.4C). Data from a center-out movement trial was used to train a naïve-Bayes classifier to distinguish, in the S1 activity (spike counts), between periods when the limb was 'moving' vs. 'not-moving'. The classifier

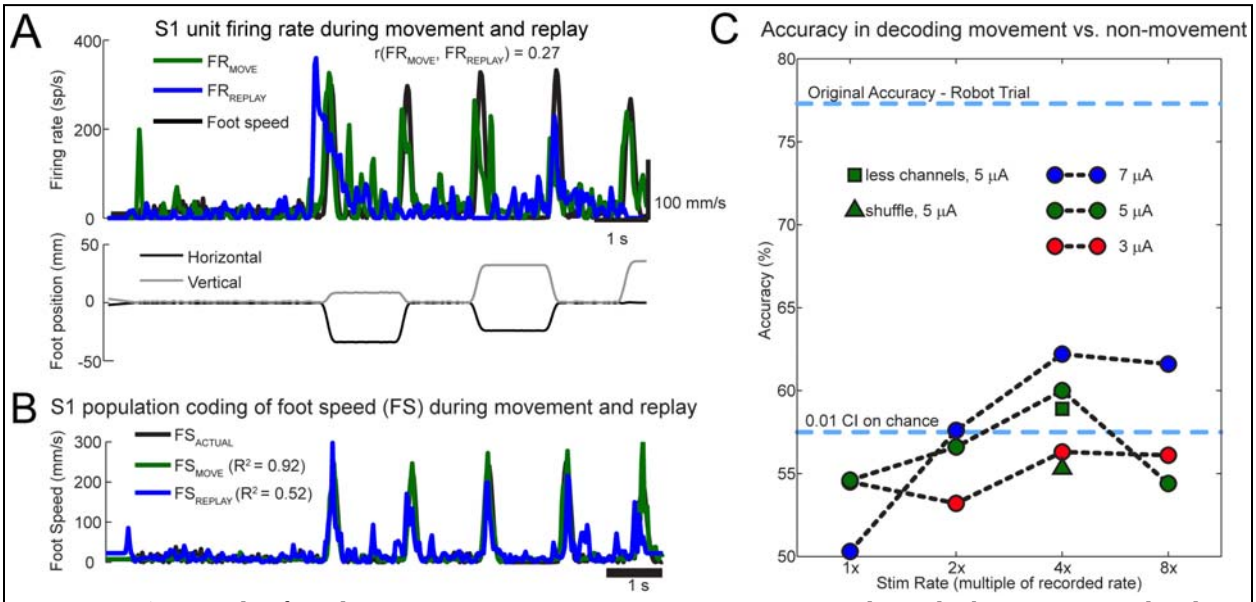

Figure 1.4: A) Example of single-unit activity in primary somatosensory cortex during limb-movement and replay PAMS. The firing rate histograms in the 2 conditions are correlated at r = 0.27. B) Decoding of foot-speed from S1 activity is similarly accurate in movement and replay conditions. C) Neural decoding classifier accuracy for replay stimulation at 1x, 2x, 4x, and 8x the original pulse-rate at 3, 5, and 7 µA stimulation intensity.

was then applied to both the original movement and replay stimulation trials. Testing replay stimulation trials using a classifier trained on robot movement data enabled classification based on features of S1 activity in the original movements. We found that increasing the amplitude and instantaneous pulse-rate of the replay stimulation resulted in classification accuracies above chance levels. Reducing the number of stimulus channels reduced the classification accuracy, but less than it was reduced when shuffling the stimulus inputs. ***The key points of this figure are: 1) replay PAMS can transmit limb-state information to S1 and 2) increasing the amplitude and instantaneous pulse-rate of replay stimulation can enhance the response.***

Response of S1 to fabricated patterns of PAMS

We are also testing the cortical response to fabricated PAMS patterns – ones that are not based on observed or modeled afferent activity. Preliminary experiments have demonstrated that certain combinations of stimulus location, amplitude and frequency can elicit discriminable responses in S1. Panel A of Figure 1.5 shows the results of a classifier trained to distinguish S1 responses (relative to baseline) to different PAMS patterns that varied in amplitude (3 – 20 µA) and location (5 different electrode pairs). Two locations (columns 1 and 4) evoked S1 responses that were classified with high accuracy (>90%) when the stimulation amplitude exceeded 7.2 µA. Accurate classification was also achieved when comparing these two channel pairs to each other (panel B). Interestingly, panel B shows a non-monotonic relationship between classification accuracy and stimulation amplitude – intensities above and below 11.5 µA were harder to discriminate. PAMS at supra-physiological frequencies (up to 1000 Hz) was also found to elicit discriminable responses in S1 (panel C). Stimulation frequency differences greater than 400 Hz were clearly distinguishable. The inset in panel C shows an example of the multiunit response to stimulation at these frequencies. ***The key point of this figure is that fabricated patterns of PAMS elicit distinguishable responses in S1 at both physiological and supra-physiological (i.e. above normal range for PA firing rates) pulse rates.***

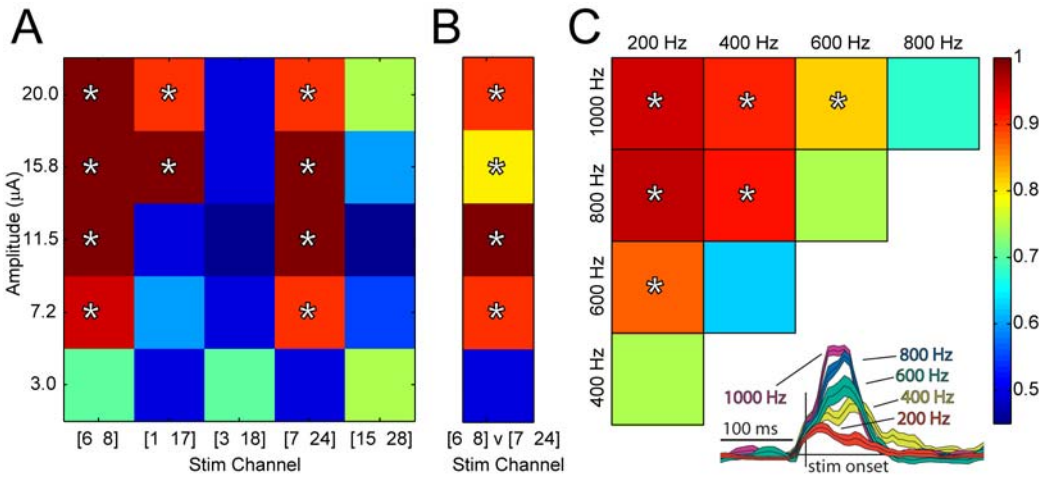

Figure 1.5: Classification accuracy for different DRG channel pairs and amplitudes: A) compared to baseline and B) between two stimulation pairs. C) Classification accuracy between S1 responses to different frequencies of PAMS. Asterisks indicate significance ($p<0.01$). Colors indicate classification accuracy.

Unexpected delays and resolutions

We have encountered some unexpected delays in our studies to evaluate the somatotopic organization of PA fibers in the DRG and spinal nerves. The problems are related to difficulty in obtaining reliable PA recordings in the rat in a way that supports an accurate reconstruction of the fiber topography. Without deviating from our stated objectives, we have decided to modify our approach slightly by using nerve tracers to track the course of nerve fibers from muscle through the spinal roots and into the spinal cord. This will allow us to precisely map the locations of muscle afferent fibers in the DRG, dorsal roots, and spinal cord. In these studies, Cholera toxin-B will be conjugated with a flourosecent die and injected into peripheral nerves for different muscle groups. The injections will trace the motor and sensory fibers for each muscle groups via retrograde transport. A new animal protocol was developed for this study and has received approval from the local IACUC. We have also submitted an ACURO protocol application and are awaiting approval. Studies will commence once we receive approval from ACURO. We will not begin these animal studies until approval of the ACURO protocol is granted.

The results from the anatomical tracing study will be used to characterize the organization and distribution of PA fibers in the DRG and dorsal roots. This information will be used to further define the geometrical properties of our computational model (i.e. the density and arrangement of PA fibers from different muscle groups). The computational model provides an accurate and detailed description of the somatotopic organization of PA fibers that can be used to simulate the effects of PAMS over a wide range of conditions. For example, the model can be used to explore a variety of electrode designs and stimulation parameters (e.g. pulse width and waveform shape) and determine, in silico, the best design for achieving selective activation of the specific PA targets.

Plans

We plan to begin testing the proposed PAMS method for providing somatosensory feedback in chronically implanted animals as soon as we receive approval from our local IACUC and the US Army ACURO. The IACUC protocol is currently under review and we expect to receive approval by mid to late February, 2010. Once the approvals are granted, we will perform chronic

implantations of DRG microelectrodes for PAMS. Cortical recordings will be made via a skull mounted chamber installed over primary somatosensory cortex, allowing reliable access for placement and manipulation of microelectrodes in primary somatosensory cortex. These studies will support the year 2 objectives, which are to evaluate 1) the amount of limb-state information that can be delivered to the brain by PAMS, and 2) reliability of this approach over an extended implant period (up to 6 months). To facilitate interpretation of these results, we will use the computational model to simulate the recruitment of PA fibers at the site of stimulation. This analysis will be used to interpret the cortical responses in the context of estimates for the number and types of fibers recruited by PAMS.

Project 2. Establishment of Neural interface stability and optimization

The implanted neural interface must remain stable throughout the lifespan of the user, but immune and inflammatory reactions at the implant site are known to degrade the performance of implanted microelectrodes. Since tissue reactions vary in different parts of the nervous system, our first objective is to compare the responses in the DRG, dorsal root nerve, and spinal cord. Our second objective is to test whether surface coating, with agents that encourage specific neuronal survival and growth and reduce inflammation, will be effective in improving the biocompatibility.

Objective 1: To compare the responses in the DRG, dorsal root nerve, and spinal cord.

We have set up a series of protocols for implantation of electrode in rat DRG and spinal cord, tissue harvesting and sectioning, staining and quantitative analysis of tissue reaction. We are in the process of completing the characterization of tissue response at 1 week and 4 week time points. Neuron-promoting coating has also been developed (described in the next section) and evaluation of the effect of these coating in vivo is also ongoing. We will describe all the established procedures and some preliminary results below.

Surgical P rocedures: All surgeries were performed under isoflurane anaesthesia. Pulse oxygenation, heart rate and end-title carbon dioxide were monitored continuously. A unilateral laminectomy was performed to expose the left side of the lumbar spinal cord and dorsal root ganglia (DRG). Up to four tungsten wire electrode tips, 2mm in length and approximately 75µm in diameter, were inserted into the spinal cord or two electrode tips were inserted into each exposed DRG. Electrode tips either had no coating or L1 coating. Following surgical implantation, the incision site was sutured closed and the rat was allowed to recover. Rats were monitored closely for signs of pain or distress and post-operative pain was managed with buprenorphine (0.3 mg/kg).

Either one week or four weeks following implantation, rats were anaesthetized with a ketamine/xylazine cocktail (100/20 mg/kg) and transcardially perfused with PBS and then 4% paraformaldehyde. The spinal cord and spinal roots were exposed, extracted and placed into a tube of 4% paraformaldehyde to post fix for up to 3 days. Tissues were then transferred to a tube of sucrose and stored for up to 1 week or until the tissue sunk to the bottom of the tube. Finally, tissues were mounted for histological analysis.

Tissue Processing: 1 week or 4 week post implantation, rats were perfused transcardially with cold PBS followed by 4% paraformaldehyde. DRG or spinal cord were exposed and removed carefully by taking off muscles and spines surround the spinal cord or DRG. Tissue was

sectioned in a cryostat at a thickness of 7 µm. HE and immunohistochemical staining of NF200, GFAP, Iba-1 and ED1 were performed for all the groups in order to detect neurons, astrocytes, microglia and activated macrophages, respectively. Double staining was performed for DRG and spinal cord with NF200 and Iba-1. To reduce the variation, all the staining were done in the same condition, i.e. same concentration of the primary and the secondary antibodies, same blocking solution and incubation time. Fluorescent images were taken using a confocal microcope at 10X.

Quantitative Image A nalysis: We are developing image analysis protocols to compare groups quantitatively. Since the expression of Iba-1 is a marker for microglia/macrophage and corresponds well to the tissue reaction, the fluorescence intensity of Iba-1 was analyzed using a custom-written MATLAB program (The Mathworks, Inc., Natick, MA) with a graphic user interface (GUI). The implantation of each electrode tip created a hole in the tissue. The edge around this hole defined the interface in polar coordinates with the center of mass of the hole defined as the origin. The intensity of each pixel in the image and each pixel's radial position relative to the edge of the interface were recorded. The intensity values were normalized with reference to background intensity. The background was defined as the average intensity of an area of pixels far from the interface. These data were tabulated, such that averaged pixel intensity was a function of radial distance from the interface, and grouped into bins of pixels every 50 µm distance from the interface.

Results

Results showed that there were cells aggregated and oriented around the electrode-tissue interface (Figure 2.1). In DRG, expression of GFAP and ED1 was very weak in both week 1 and 4 (not shown). In spinal cord, the expression of GFAP showed aligned fiber-like morphology which are disrupted by the electrode (Figure 2.1, right) and the expression of ED1 were slightly activated (not shown). The GFAP reaction is distinctly different from that in the brain tissue where a significantly elevated level of GFAP will be found around the hole suggesting glial scar. The expression of Iba-1 was activated by electrodes both in DRG and in spinal cord, while NF200 staining (stained both axons and cell body in DRG, but only axons in SI) was disturbed and lost near the electrode-tissue interface (Figure 2.2, 2.3). We do not have enough sample size currently to make any conclusion about the comparisons, but preliminarily, the L1 coating has decreased the Iba-1 reaction both at 1 week in DRG and 4 weeks in SI (Figure 2.3, 2.4).

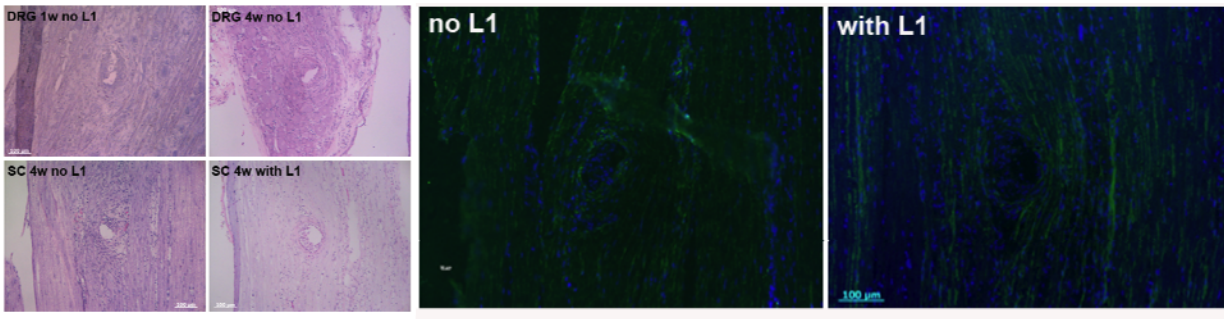

Figure 2.1. Left: H&E staining of the tissue around the implants with and without L1 coating at 1 and 4 weeks. H&E staining shows aggregation of cells surrounding the implant. Right: GFAP staining (green) of spinal cord around implant with and without L1 coating at 4 weeks. Blue stains nuclei.

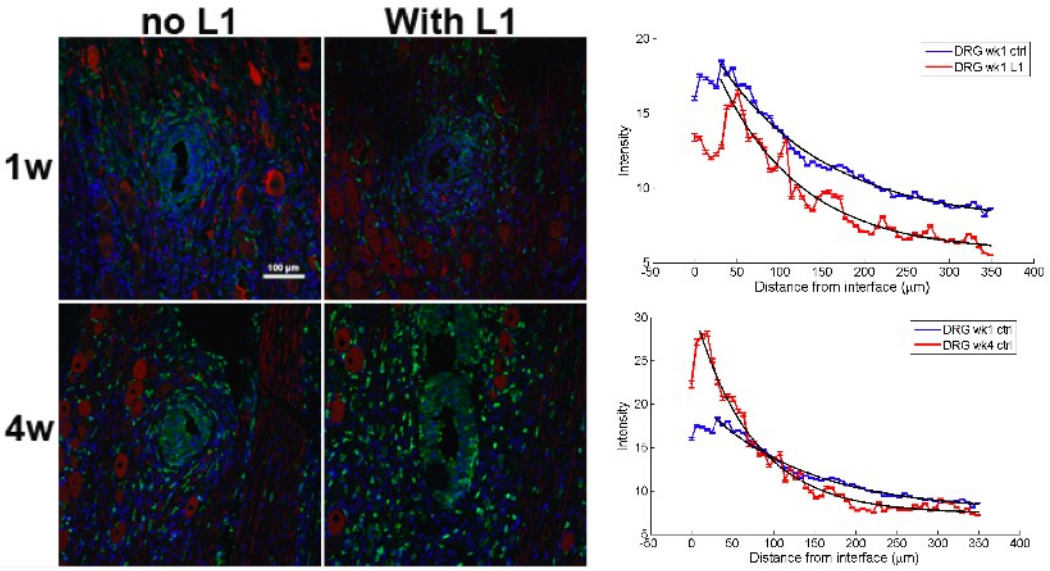

Figure 2.2: Fluorescent images of DRG tissue around the implants with and without L1 at week 1 and 4. Blue nuclei, red Iba-1 and green NF-200. On right, example of quantification of Iba-1 intensity over distance. Week 1 from the average of 3 implants and week 4 from one implant.

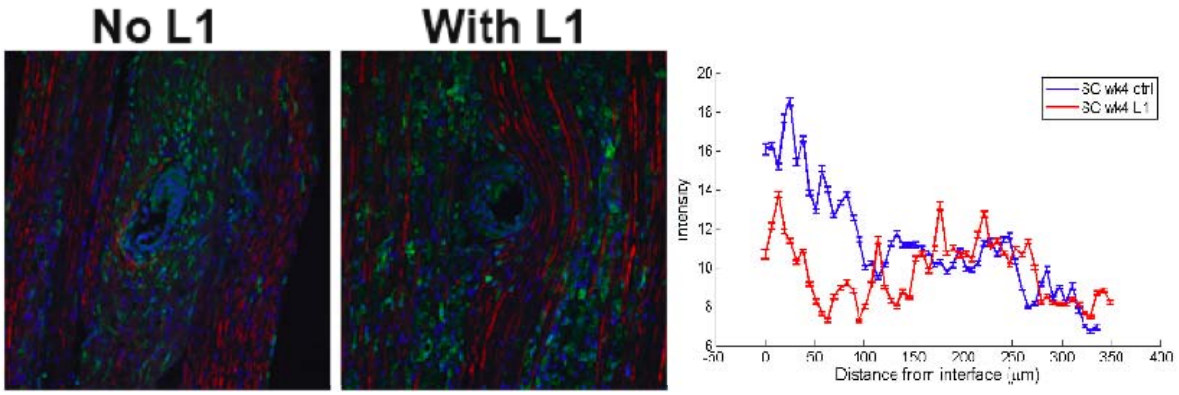

Figure 2.3: Representative images of NF200/Iba-1 staining for spinal cord 4 weeks post implantation with uncoated or L1 coated electrode. Iba-1 fluorescence intensity was reduced with L1 coated electrode.

Plans

There are clearly other cells at the vicinity of the holes that are not Iba-1, NF-200 and GFAP positive. Next, we plan to stain vimentin and fibronectin to identify fibroblasts, S100 to identify schwann cells, in order to obtain a complete picture of the tissue response. In the next stage, we plan to complete all the implantations, refine the image analysis tools and summarize the results in one or two manuscripts.

Objective 2: To test w hether surface c oating, w ith agents that encourage specific neuronal survival and grow th and reduce infl ammation, will be effective in im proving the biocompatibility

Two types of coatings are being developed for the electrodes, one is for surface immobilization of neural adhesion molecules and the other is for the controlled release of anti-inflammatory drugs. The effect of these coatings on cells and tissue are being characterized.

A. Surface immobilization of neural adhesive molecule. The surface of parylene C (insulating layer of the FMA electrodes) is coated with neural adhesion molecule L1, which specifically promote neuronal health, neurite outgrowth while inhibiting glial cells. The coating condition was developed in year 1. In year 2, we have completed the full in vitro characterization and began to evaluate the effect of L1 coating *in vivo*.

Parylene C wires that are used in the assembly of the FMA electrodes were cut to be approximately 0.5-1cm long during *in vitro* experiments. Parylene C wires were coated with L1 and laminin (positive control) following an established protocol by our lab. Briefly, the Parylene C wires were plasma treated for 10 seconds and immersed in either 100 µg/ml of L1 or 40 µg/ml of laminin protein solutions for 1 hour and followed by a PBS rinse. All conditions, (untreated wires, plasma treated wires, and protein (L1/laminin) coated wires) were mounted on round glass coverslips using KwickSil and placed in 24 well cell culture plates (Costar). To observe the effect of the L1 protein and its bioactivity while its present on the surface of the wire, three primary cell types (neurons, astrocytes, and microglia) were chosen for the *in vitro* experiments. Seven samples per treatment condition were tested for each cell type (n=7).

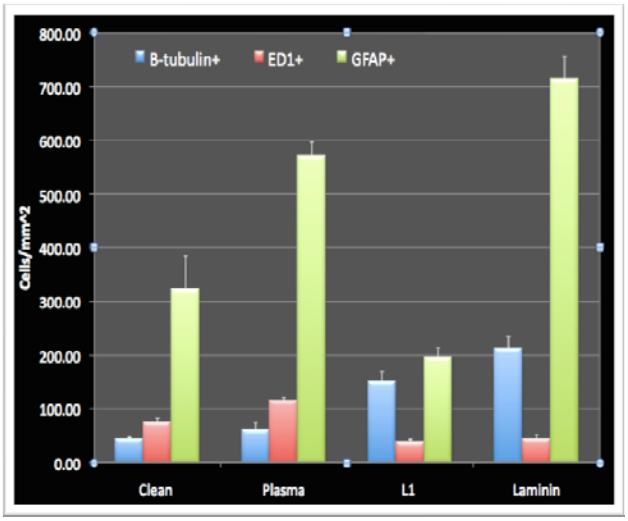

Figure 2.4: Data representing cell attachment and growth per surface area on untreated and modified Parylene C wires. L1 treated wires showed a significant difference when compared to the untreated wires *p<0.05. β-tubulin III stains for neurons, ED1 stains for activated microglia, and GFAP stains for astrocytes

The quantitative cell counts are summarized in Figure 2.4. Number of neurons increased on both types of wires with the L1 and laminin coating, while the number of activated microglia decreased on both L1 and laminin coating. Between the L1 and laminin coatings, there are significantly less astrocytes on the L1 coated wires than the laminin coated wires. This is expected based on the different bioactivities of the two proteins. L1 is a neuron specific adhesion molecule that promotes neuron growth and adhesion via homophilic binding, while laminin is an extracellular matrix protein that can bind to many types of cells. These results suggest that our coating technique is reliable in immobilizing L1 and laminin proteins with high bioactivity. Furthermore, the L1 coating showed the most desired properties for improved neural tissue interface.

B. Controlled release of anti-inflammatory drug.

We continue to apply nanotechnology to this research. After developing a nano-porous film of polypyrrole with enhanced drug load and release efficiency as reported last year, we have developed a layered nanostructure (a sponge like nanostructure film). The nanostructured PPy film was composed of template-synthesized nanoporous PPy covered with a thin protective PPy layer. The system can load drug molecules in the polymer backbones and inside the nanoholes respectively. Electrical stimulation can release drugs from both the polymer backbones and the

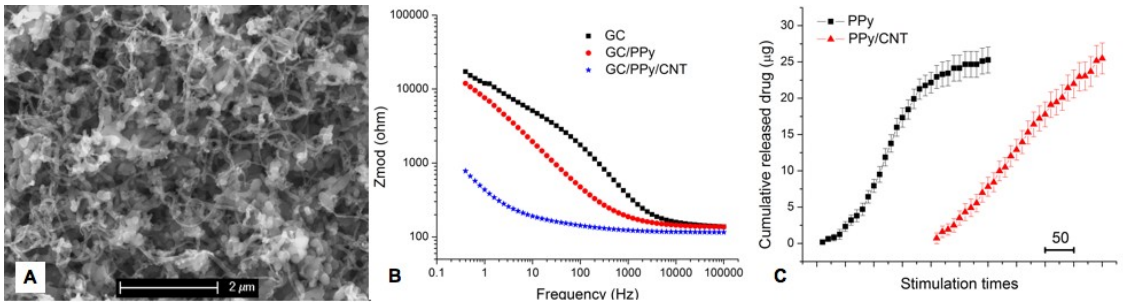

Figure 2. 5: (A) Scanning Electron Microscopy of PPy/CNT film. CNT's outer diameter 20-30 nm, inner diameter 5-10 nm. The shapes of carbon nanotubes are clearly seen and PPy grows around the tube encapsulating the drugs inside. (B) Electrochemical impedance spectroscopy (EIS) of bare, PPy and PPy/CNT coated GC electrodes. The EIS was measured in a solution containing 5 mM $[Fe(CN)_6]^{3+/4+}$ and 0.1 M KCl. (C) Drug releasing profiles for 300 stimulation times. Each time the stimulation applied was -0.5 V for 5s followed by +0.5 V for 5 s.

nanoholes, which significantly improves the drug load and release efficiency. Furthermore, with one drug incorporated in the polymer backbone during electrochemical polymerization, the nanoholes inside the polymer can act as containers to store a different drug, and simultaneous electrically triggered release of different drugs can be realized with this system. This work has been published in Electrochemical Communication [new publication by Luo and Cui, see "REPORTABLE OUTCOMES"]. More recently, we have introduced carbon nanotubes (CNTs) to the polymer film. CNTs function as drug nanoreservoirs which can effectively store drug molecules and release them upon electrical stimulation and the release profile is more linear and sustainable than previously reported PPy based electrically controlled release systems (Figure 2.5).

One common concern with CNT is its toxicity. Cell cultures were used to verify that CNTs are not toxic. Neurons and astrocytes have been successfully cultured on various PPy/CNT films and healthy growth for both cell types were observed (Figure 2.6). A negative relationship between film roughness and culture health was found. In addition, dexamethasone has been released from films in culture using an applied electrical stimulation. Preliminary results indicate that the effect of the stimulus current had no negative impact on culture health, and that the impact of released dexamethasone has a comparable effect on neurons as dexamethasone added in solution directly to the neuron culture. Future studies will further explore and quantify the impact of stimulated dexamethasone release on neuron and astrocyte cultures.

Plan

We will continue to test the plasma+L1 coating treatment *in vivo* and the tissue response will be compared to the non-treated electrodes. For the controlled release coating, we will finish the *in vitro* Dex release studies to find the optimal release condition in cell culture. Then the

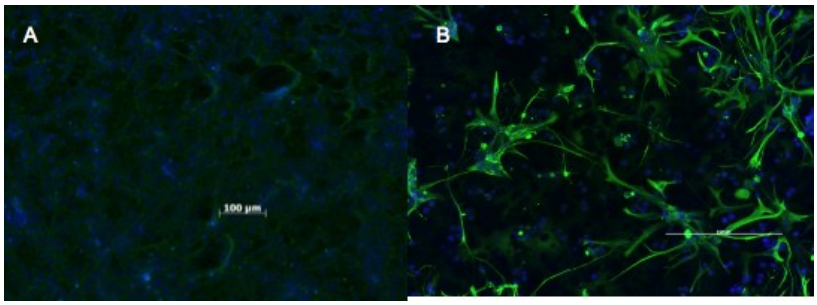

Figure 2.6: (A) Neurons cultured on polypyrrole with MWCNTs and SDS, without dexamethasone, 30s coating. Thin, uniform film allows for confluent neuron growth, similar to plain gold surface. Blue = DAPI, Green = anti-TuJ1. Scale = 100μm.(B) Image 2: Astroglia cultured on polypyrrole with MWCNTs, SDS, and dexamethasone, 30s coating. Blue = DAPI, Green = anti-GFAP. Scale = 500μm.

electrically controlled drug releasing coating will be applied on electrode arrays and the effect of drug release in minimizing inflammatory tissue reaction in the animals will be characterized.

Project 3. Virtual reality environment for prosthetic training and testing

Objectives

A virtual environment will be created that will allow amputees to: 1) test simulated neuroprosthetics and control algorithms, and 2) practice using the neuroprosthetic in a virtual training environment. The main objective for the FY06 funding period is to design, acquire, and assemble a virtual reality system for training people to use an upper extremity neuroprosthesis (months 1-6). In months 3-12, we will develop and test the VR system with myoelectric control inputs, and test the system with upper extremity amputees performing simulated reaching tasks.

In FY07 we will further refine our VR training system and optimize the use of myoelectric signals for controlling specific natural tasks for which they may be best suited, natural grasping and pinching movements. In addition, we will use direct brain interface (DBI) signals, such as magnetoencephalography (MEG) and electrocorticography (ECoG) to control a virtual hand. We will also explore how these signals can be used interactively with EMG signals. The ultimate goal is to develop a DBI or hybrid EMG-DBI system that persons with high-level spinal cord injury can use to regain motor function.

Results

Approval from both the U.S. Army HRPO and University of Pittsburgh IRB

We have successfully secured approval from both the Army Human Research Protection Office (HRPO) and the University of Pittsburgh Institutional Review Board to conduct human studies in both able-bodied individuals and individuals with limb amputations. Initial pilot testing of the system has been completed, and we are now ready to recruit subjects to participate in this study.

Fully-functional virtual reality (VR) simulator system for prosthetic control training

We have developed a fully-functional virtual reality simulator using a combination of BCI2000 software and the Matlab/SIMULINK Virtual Reality Toolbox. This VR environment includes simulated prosthetic hands and virtual objects. We have developed behavioral testing paradigms using this VR simulator to simulate virtual grasping and pinching movement. Figure 3.1 shows the basic system architecture.

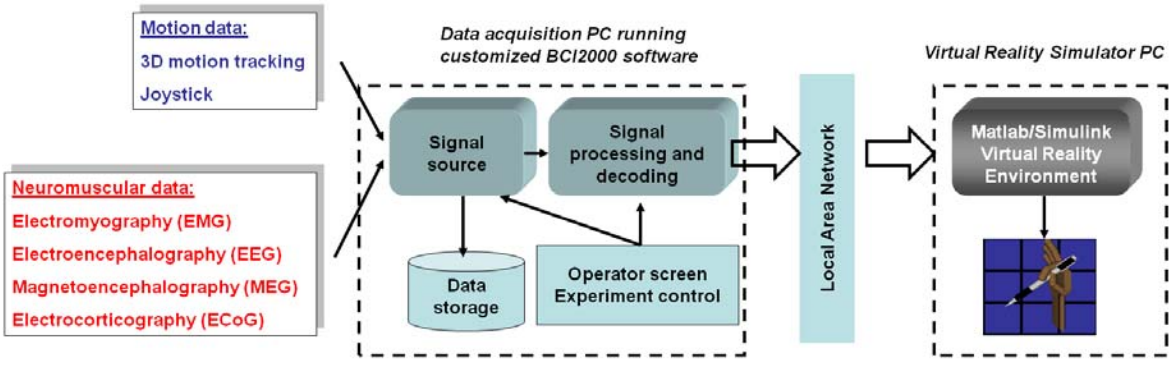

Figure 3.1: Basic layout of the virtual reality neuroprosthetics user training system architecture. This design uses BCI2000 software as the base to acquire myoelectric and neural signals. On top of BCI2000, we developed a virtual reality (VR) simulator for virtual prosthetic hand control training. BCI2000 and virtual reality simulator run on two separate computers connected through the LAN within the lab, but they can also be distributed across the internet.

Develop and testing of a novel synergy-based prosthetic hand control scheme

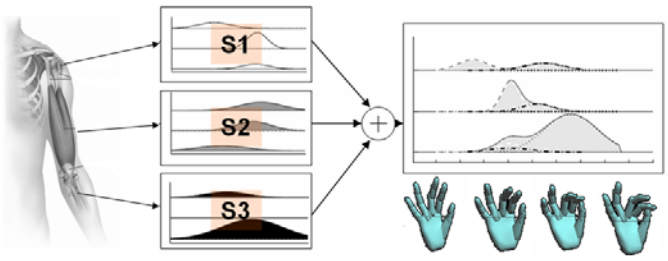

Figure 3.2: A novel synergy-based myoelectric control of dexterous prosthetic hand.

We have proposed and implemented a novel prosthetic hand control scheme, which is called the synergy-based control. This is based on previous studies in human hand movement dimension techniques (Vinjamuri et al. 2009). The synergy model can effectively reduce high-dimensional dexterous hand movement (with more than 17 degrees of freedom) into only 3 synergy control signals (3 degrees of freedom). This allows us to control dexterous prosthetic hands with a very small number of independent control signals obtained through either surface EMG recording or direct brain interface systems. Figure 3.2 shows the basic concept of the synergy-based control scheme. Briefly, each synergy represents a movement primitive, such as grasping or pinching movement. Each synergy is represented by movement across all 10 different hand and finger joints with a very short period of time (e.g. 0.5 to 1 sec). These synergies serve as basic kernels, and three independent control signals will be convolved with those three synergies leading to smooth time-varying hand movement across all 10 joints of the virtual prosthetic hand. Figure 3.3 demonstrates the feasibility for controlling prosthetic hand to perform pinching and grasping movement using two independent control signals. In this case, we used two cortical surface electrodes to record the electrocorticographic (ECoG) signals for controlling the virtual hand.

Modification of current protocol for including MEG component

In addition to the original objectives, we would like to include a magnetoencephalography-based brain computer interface (MEG-BCI) component. The aim of Project 3 in FY06 is to use a virtual reality environment to increase EMG activity in the residual limb for myoelectric prosthetic control. In FY07, the next step is to test the effect of virtual reality (VR) training on direct brain interface control. Originally, we proposed to study this effect in individuals with ALS using brain signals captured with a direct brain interface (DBI). However, the success of complementary research using MEG provides us a new opportunity to study this effect in control subjects as well as upper limb amputees. MEG is a non-invasive whole-head neural recording method that offers high spatial and temporal resolution. We would like to add a MEG-BCI component so that VR testing can be completed in the targeted group of users: upper limb amputees. MEG recordings will be recorded and used for real-time control of a virtual limb. The MEG system also allows for simultaneous recording of EMG so a hybrid MEG/EMG-BCI could be implemented. We believe that the addition of MEG to this protocol provides substantial benefits. First, MEG provides a non-invasive way to localize brain areas that are responsible for overt or intended movement. By co-registering MEG data with a structural MRI of the brain, we can measure the location and size of activity sources within the brain. In this way, MEG could act as a screening tool to determine the optimal site for implantation of a DBI device. Second, we will be able to provide real-time feedback of both EMG and neural signals in the context of a virtual reality environment which will likely accelerate the plasticity mechanisms within the nervous system. We hope that this leads to better prosthesis control as reorganization will occur through two pathways, both the peripheral and central nervous system. Third, we will

be able to test the EMG and MEG-based training paradigms with all of our participants including control subjects and upper limb amputees. We plan to perform MEG-BCI training in 10 subjects.

Development of real-time MEG software

Magnetoencephalography (MEG) is a non-invasive way to study brain functions with high temporal resolution. There is an emerging interest in studying the potential use of MEG for brain-machine interface (BMI). To date, the majority of studies have performed offline analysis to reveal detailed information about the spatial and temporal evolution of neural activity as it relates to a task, or to measure neuroplasticity resulting from an intervention. However, real-time feedback of this activity could benefit many areas of research, including BMI. Currently there is no available method to capture the large amount of information from a 306-channel Elekta Neuromag® MEG system in order to provide real-time feedback. We have developed a toolbox that can stream in real-time MEG signals from this system to any computer. These signals can be processed with minimal delay (<30 ms) and used for different types of applications. Our MEG toolbox is integrated with BCI2000, a widely used open source software package for BMI research and development [1], and it can be easily configured to relay the real-time signal in

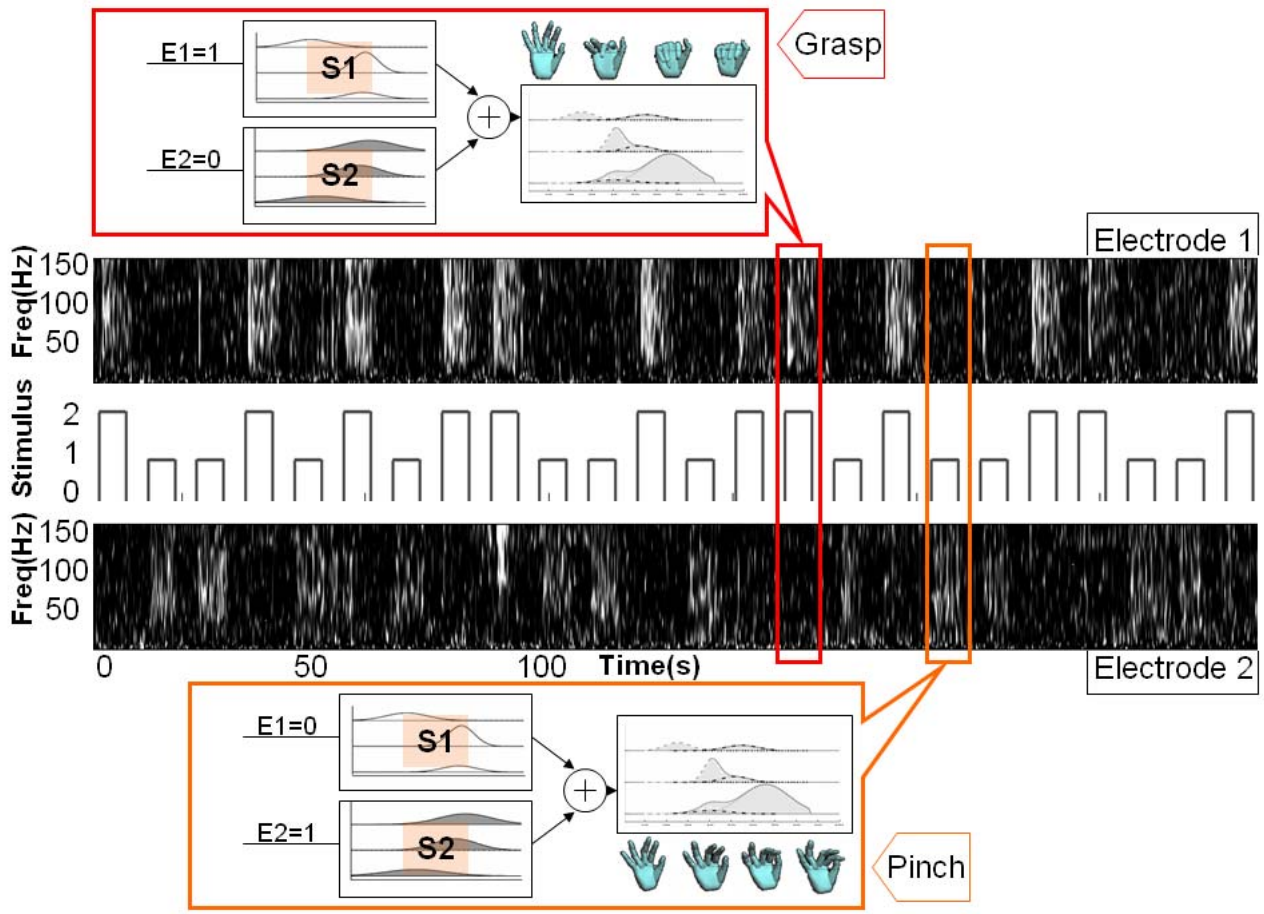

Figure 3.3: Demonstration of real-time control of dexterous virtual hand movement using the synergy-based control scheme. The two gray-scale plots (labeled as Electrode 1 and 2) show the spectrograms of two independent ECoG channel, and the gray-scale represents percentage change from baseline. Whiter means higher band power. The red and orange rectangle specifically marked two sample trials where the subject controlled the virtual hand to either grasp or pinch a virtual object.

binary format to any arbitrary host in the network. Preliminary results indicate that we can achieve a frame-rate of approximately 35 Hz with 324 channels of data sampled at 1000 Hz, which is sufficient for many real-time BMI studies. This real-time software can be a valuable tool for real-time BMI research, for stroke and spinal cord injury rehabilitation through real-time neurofeedback paradigms, and for neuroscience research in general. The toolbox will be made available to the scientific research community as open source along with the BCI2000 software, and we hope that it can open new possibilities for the many areas of research using MEG.

Plans

We will further refine our virtual hand simulation system to include richer behavioral tasks and better integrate it with our DBI recording systems for MEG and ECoG-based control. We will also start recruiting both non-impaired individuals and those with amputees and examine the effectiveness of our synergy-based control scheme and our virtual training environment.

Project 4. **Prosthetic hardware testing**

Objectives

Little objective or validated information exists about the quality and functional reliability of prostheses. The primary objective for the FY06 funding period is to develop and assemble a testbed for life-cycle testing of a variety of prosthetic feet. In months 1-6, we will design the testing apparatus and acquire and assemble the hardware and software for testing. We will also complete pilot testing with a small number of prosthetic limbs to validate the system.

In FY07, we will use the testbed to perform life-cycle testing of a variety of prosthetic feet. In months 1-6, we will acquire representative samples of the most popular foot designs and create fixturing for attaching the feet to the testbed. In months 3-12, we will perform the life-cycle testing and analyze the data.

Results

Acquire prosthetic feet and completed pilot testing: Prosthetic feet from three different manufacturers was ordered. The feet being tested are as follows: three Freedom 1000 Sierras, three Ossur Reflex VSPs, and three Ohio Willow Wood Pathfinders (Table 1). Technical issues with the machine were resolved and pilot testing with a Freedom 1000 Sierra was completed. Pilot testing was done on actual specimens; starting with a Freedom 1000 Sierra at P3 loading level. This first test was completed successfully. Other feet will be tested at the P5 loading level. During the testing, position and force data was collected for each channel (heel and forefoot). This data will allow us to compare feet on the basis of creep rate and hysteresis, along with pass and fail. A data analysis program was developed to calculate these parameters.

Procurement: All Prosthetic feet from three different manufacturers were received including Freedom FS Sierras, Ossur VSPs, and Ohio Willow Wood Pathfinder II. Teflon sheets and Teflon tape were also purchased. Teflon was used on the bottom of the loading surface of the plates on both actuators so that load application at foot was frictionless.

Testing with P5 loading level: During the static proof tests, a maximum force of 2240 N is applied in a downward direction for 30 seconds on the heel and forefoot consecutively. During the ultimate strength tests, force is applied separately on the heel and forefoot, increasing gradually from 3360N to 4480 N at the rate of 175N/ 20 seconds. During the fatigue tests, load is applied on both the heel and forefoot alternatively for 2,000,000 cycles at a frequency of 1 Hz followed by a final static proof test at the P5 loading level. Each foot is examined before and after every test and often during the fatigue test.

Preliminary result: ISO 10328 test with P5 loading level was completed on Pathfinder II and VSP re- flex. VSP re-flex feet completed the test successfully without any deformation or fracture. Pathfinder II passed the proof test and ultimate test but failed during the fatigue test at 274,778 cycles. There was hairline fracture at both sides of the upper part of foot plate. Fatigue testing is in progress on 2nd foot from Freedom 1000 Sierra. Proof and ultimate test was completed on this 2nd freedom foot.

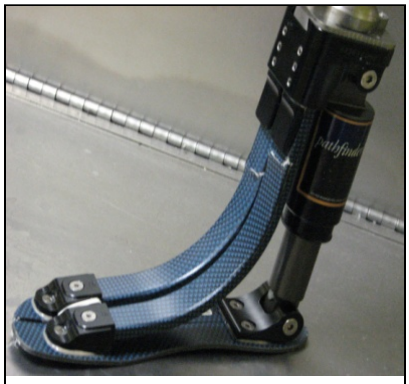

Figure 4.1: Hairline fracture in Pathfinder

Figure 4.2: Freedom Sierra FS1

Figure 4.3: Ossur Re-flex VSP

Table 4.1: Characteristics of prosthetic feet tested

Manufacturer	Model	Activity level	size	Material	category	Weight limit
Freedom	Sierra FS1	High	26 cm	Carbon fiber	9	365lbs
Ohio Willow Wood	Pathfinder II	High	26 cm	Carbon fiber& pneumatic heel spring	9	350 lb
Ossur	Re-flex VSP	High	26 cm	Carbon fiber &compression spring	9	365lbs

High activity level include rigorous activity, competitive sports, running, power lifting, snowboarding

Table 4.2: Test Results

Foot model	Proof test	Ultimate test	Fatigue test	Test results
Sierra FS1	Passed	Passed	Passed	No fracture/ deformation
Pathfinder II	Passed	Passed	Failed at 2,74778 cycle	Hairline Fracture
Re-flex VSP	Passes	Passed	Passed	No fracture/ deformation

Plans:

Continue testing the 6 remaining feet from three different manufacturers at ISO Standard P5 loading level.

Table 4.3: Time frame and Schedule for remaining six feet

Testing Schedule	2009: Test completed					2010: Deadlines for testing					
	August	September	October	November	December	January	February	March	April	May	June
Freedom Sierra FS1	Pilot testing	Done		Technical problem		Testing			Will be tested		
Ohio willow wood Pathfinder			Done					Will be tested		Will be tested	
Ossur Re-flex VSP				Waiting for Foot	Done		Will be tested				Will be tested

Figure 4.4: Material Testing System (MTS) with two uniaxial actuators. Both actuators used for testing purpose

Key Research Accomplishments

Project 1. Develop a somatosensory neural interface (SSNI)

Milestones	Progress
Characterize somatotopic organization in DRG and dorsal roots	• Reliable afferent recordings have been difficult to obtain in rat DRG and dorsal roots. A neuro-tracing study has been designed to fulfill this objective – pending ACURO approval. • Microstimulation studies have revealed that a range of sensory modalities can be recruited at low stimulation intensities in the DRG, and similarly in the dorsal roots and spinal cord (Figure 1.1). • A computational model of the DRG and dorsal root fiber organization and recruitment by electrical stimulation has been constructed (Figure 1.2)
Afferent microstimulation and cortical recording experiments	• Primary afferent microstimulation (PAMS) evokes 'proprioceptive' neuronal responses in the brain that are similar to those evoked by movement of the leg (Figure 1.4A,B) • Increasing the intensity or rate of stimulation enhances the proprioceptive responses in the brain (Figure 1.4C). • Artificial or 'fabricated' patterns of PAMS elicit distinguishable responses in the brain at both physiological and supra-physiological (i.e. above normal range for PA firing rates) pulse rates (Figure 1.5). These experiments reveal the stimulation parameters that are most effective (and least effective) for eliciting responses in the brain.
Chronic stimulation and recording experiments	• Animal protocol is under review by Pitt IACUC; once approved, a submission to ACURO will follow. Experiments will start in Spring, 2010.

Project 2. Establishment of Neural interface stability and optimization

Milestones	Progress
Microelectrode array implant surgeries with treated and untreated electrodes.	• Developed and tested the L1 and Dexamethasone releasing coating for the parylene C insulated electrodes.
Histological evaluation of implant sites	• Half way through the in vivo experiments on evaluating the tissue response to electrodes implanted chronically in DRG and spinal cord.
Implant surgeries for tissue reaction to chronic stimulation study.	• These studies will be performed in conjunction with the chronic stimulation and recording experiments in Project 1.
Histological evaluation of implant sites	Not started.

Project 3. Utilization of a virtual reality environment for prosthetic training and testing

Milestones	**Progress**
Acquire and configure hardware for VR system	• Completed
Develop VR training environment with myoelectric inputs	• Completed
Test and refine VR system with upper extremity amputees	• We have obtained human study approval from both the U.S. Army Human Research Protection Office and the Institutional Review Board (IRB) at the University of Pittsburgh. • We have conceived and implemented a novel prosthetic control scheme based on the concept of hand movement synergies, which allows us to control multiple degrees of freedom dexterous hand movement using a very small number of myoelectic or neural signals. • We'd like to thoroughly test our VR systems in non-impaired individuals before we start recruiting individuals with upper extremity amputation. But we plan to start recruiting individuals with amputations in FY07
Use direct brain interface (DBI) signals to control virtual arm; integrate DBI and EMG for control.	• We have demonstrated that a DBI based on electrocorticography (ECoG) signals recorded from a human subject can be used to control the movement of a virtual hand. • We have requested project modification to further include the MEG component. • We have finished the first iteration of modification for our current MEG research protocol so that it can be approved by the U.S.Army (HRPO) and the IRB office at the university.

Project 4. Prosthetic hardware testing

Milestones	**Progress**
Design and assemble system for prosthetic life-cycle testing.	• Complete.
Develop data acquisition system and complete pilot testing	• Complete
Acquire prosthetic feet and develop fixturing for life-cycle testing	• Ongoing
Complete testing of prosthetic feet.	• Ongoing

REPORTABLE OUTCOMES

Project 1. Develop a somatosensory neural interface (SSNI)

[1] S. W. Brose, D. J. Weber, B. A. Salatin *et al.*, "The Role of Assistive Robotics in the Lives of Persons with Disability," *American Journal of physical medicine & rehabilitation*, in press.

[2] D. J. Weber, L. M. Miller, J. K. Chapin *et al.*, "Practical considerations for the location and design of a somatosensory neural interface.," in Smart Sensorimotor Prosthetics, Washington, DC, 2009.

[3] D. Weber, G. Loeb, J. T. Francis *et al.*, "Sensible Neuroprosthetics."

[4] J. B. Wagenaar, V. Ventura, and D. J. Weber, "Improved decoding of limb-state feedback from natural sensors," *Conf Proc IEEE Eng Med Biol Soc,* vol. 1, pp. 4206-9, 2009.

[5] J. B. Wagenaar, V. Ventura, and D. J. Weber, "Improved decoding of limb-state using feedback from natural sensors." p. 175.11/Z38

[6] J. B. Wagenaar, R. A. Gaunt, V. Ventura *et al.*, "Feedback Control of FES by Online Decoding of Limb-Position from the Firing Rates of Muscle and ". pp. OP-9-1-7A.

[7] M. G. Perich, J. A. Hokanson, R. A. Gaunt *et al.*, "Improving Limb-State Decoding Using a Liquid State Machine ".

[8] J. A. Hokanson, and D. J. Weber, "Using Classifiers to Identify Differences in Evoked Responses from Stimulation of Primary Afferents ". pp. OP-10-1-8B.

[9] R. A. Gaunt, J. A. Hokanson, and D. J. Weber, "Microstimulation of primary afferent neurons in the L7 dorsal root ganglia using multielectrode arrays in anesthetized cats: thresholds and recruitment properties," *J Neural Eng,* vol. 6, no. 5, pp. 55009, Oct, 2009.

[10] D. J. Bourbeau, and D. J. Weber, "Hindlimb Endpoint Forces Evoked by Microstimulation of Ventral Root Nerves in Rat." pp. PS-9A-113.

Project 2. Establishment of Neural interface stability and optimization

1. Xiliang Luo, Xinyan Tracy Cui, Sponge-like nanostructured conducting polymers for electrically controlled drug release, Electrochemistry Communications Volume 11, Issue 10, October 2009, Pages 1956-1959
2. Erdrin Azemi, Glenn T. Gobbel and Xinyan Tracy Cui "Seeding neural progenitor cells on silicon based neural probes", accepted by Journal of Neurosurgery.
3. T. W. Sleight, X. Cui E. Azemi, and D. Weber Quantification of Chronic Microelectrode Signal Quality over Time. *Poster Presentation*, Biomedical Engineering Society (BMES) Annual Meeting, Pittsburgh, PA. October 6-9, 2009.
4. Xiliang Luo, Xinyan Tracy Cui. Electrochemically Controlled Drug Release Based on Nanoporous Conducting Polymer Polypyrrole. 2009 Materials Research Society Spring Meeting, San Francisco, CA, April 13-17, 2009.
5. Xiliang Luo, Xinyan Tracy Cui. Enhanced Electrically Controlled Drug Release Using Carbon Nanotubes Doped Conducting Polymers. 2009 BMES Annual Meeting, Pittsburgh, PA, October 7-10, 2009.
6. Erdrin Azemi, Douglas Weber, Carl Lagenaur, Xinyan Tracy Cui. "Parylene C surface modification with L1 for a more biocompatible chronic cortical implant."*Poster Presentation*, Biomedical Engineering Society (BMES) Annual Meeting, Pittsburgh, PA. October 6-9, 2009.

Project 3. Utilization of a virtual reality environment for prosthetic training and testing

The above work has led to multiple journal and conferences papers, as well as conference presentations at Society for Neuroscience, Biomedical Engineering Society, and etc. All the journal and conference papers have been attached to this annual report.

1. Collinger JL, Degenhart AD, Boninger ML, Vinjamuri R, Sudre G, Tyler-Kabara EC, Weber D, Wang W (2009) Directional response of micro-ECoG recordings during a non-structured center-out task. In: BMES Annual Fall Scientific Meeting. Pittsburgh, PA.
2. Collinger JL, Wang W, Degenhart AD, Vinjamuri R, Sudre GP, Tyler-Kabara EC, Weber DJ, Wang W (2009) Towards a direct brain interface for controlling assistive devices. In: International Symposium on Quality of Life Technologies. Pittsburgh, PA.
3. Collinger JL, Wang W, Vinjamuri R, Degenhart AD, Sudre GP, Boninger ML, Tyler-Kabara EC, Weber DJ (In Review) Mirror Neuron-Like Response of Electrocorticographic Recordings During Overt and Observed Hand Movement. International Journal of Human Computer Interaction.
4. Degenhart AD, Collinger JL, Vinjamuri R, Sudre GP, Leuthardt E, Moran DW, Boninger ML, Schwartz AB, Crammond DJ, Tyler-Kabara EC (2009) Decoding finger movement from human cortical activity recorded using micro-electrocorticography. In: BMES Annual Fall Scientific Meeting. Pittsburgh, PA.
5. Degenhart AD, Pomerleau DA, Mitchell T, Gaunt R, Sudre GP, Collinger JL, Vinjamuri R, Weber DJ, Wang W, Tyler-Kabara EC (2009) Cortical representation of conceptual knowledge recorded using elctrocorticography. In: Society for Neuroscience. Chicago, IL.
6. Guo C, Li X, Taulu S, Wang W, Weber DJ (In Press) Real-time robust signal space separation for magnetoencephalography. IEEE Transactions on Biomedical Engineering.
7. Pan J, Sudre G, Palatucci M, Gaunt R, Wang W, Pomerleau DA, Mitchell T (2009) Decoding cognitive state using magnetoencephalography. In: BMES Annual Fall Scientific Meeting. Pittsburgh, PA.
8. Sudre G, Pomerleau DA, Weber D, Wang W, Mitchell T (2009) MEG Analysis of spatiotemporal activation in semantic representation task. In: Society for Neuroscience. Chicago, IL.
9. Vinjamuri R, Degenhart AD, Collinger JL, Sudre GP, Crammond DJ, Tyler-Kabara EC, Weber DJ, Wang W (2009) Decoding hand posture based on human micro-electrocorticographic signals recorded during action observation. In: Society for Neuroscience. Chicago, IL.
10. Vinjamuri R, Degenhart AD, Collinger JL, Sudre GP, Leuthardt E, Moran DW, Boninger ML, Schwartz AB, Crammond DJ, Tyler-Kabara EC, Weber DJ, Wang W (2009) Human micro-electrocorticographic signals recorded during action execution and observation. In: BMES Annual Fall Scientific Meeting. Pittsburgh, PA.
11. Vinjamuri R, Degenhart AD, Collinger JL, Sudre GP, Adelson PD, Holder DL, Boninger ML, Schwartz AB, Crammond DJ, Tyler-Kabara EC, Wang W (2009) A fuzzy logic model for hand posture control using human cortical activity recorded by micro-ECoG. In: IEEE EMBC. Minneapolis, MN.
12. Wang W, Degenhart AD, Collinger JL, Vinjamuri R, Sudre GP, Adelson PD, Holder DL, Leuthardt E, Moran DW, Boninger ML, Schwartz AB, Crammond DJ, Tyler-Kabara EC, Weber DJ (2009) Human motor cortical activity recorded with micro-ECoG electrodes

13. Wang W, Collinger JL, Perez MA, Tyler-Kabara EC, Cohen LG, Birbaumer N, Brose SW, Schwartz AB, Boninger ML, Weber DJ (2010) Neural interface technology for rehabilitation: exploiting and promoting neuroplasticity. Phys Med Rehabil Clin N Am 21:157-178.
14. Wang W, Sudre GP, Kass RE, Collinger JL, Degenhart AD, Bagic AI, Weber DJ (In Preparation) Decoding and cortical source localization for intended movement direction with MEG. J Neuroscience.
15. Zhang J, Sudre G, Li X, Wang W, Weber D, Bagic A (In Preparation) Group independent linear discriminant analysis for magnetoencephalography-based brain computer interfaces. IEEE Transactions on Biomedical Engineering.

Project 4. Prosthetic hardware testing

A poster was presented on "Protocol Development for Prosthetic Feet Testing Standards" at State of Science Symposium on Regenerative Rehabilitation at Walter Reed Army Medical Center. Many clinicians and prosthetic professionals were curious to know the outcome of this study. Another paper was submitted on "Mechanical Testing of Heavy Duty Prosthetic Feet" for RESNA 2010 conference proceedings. This paper was descriptive in the nature including preliminary analysis of present result.

1. **Kumar A, Pearlman J, Mason Z, Hong EK, Laferrier J, Cooper R and Cooper RA.** Development of Protocol for Prosthetic Feet Testing Standards. In: State of Science Symposium on Regenerative Rehabilitation at Walter Reed Army Medical Center November 13, 2009

2. **Kumar A, Pearlman J, Mason Z, Karmarkar A, Cooper R and Cooper RA**. Mechanical Testing of Heavy Duty Prosthetic Feet. Submitted manuscript for RESNA 2010 Annual Conference.